

SCENARIOS OF GIANT TSUNAMIS OF TECTONIC ORIGIN IN THE MEDITERRANEAN

Stefano Tinti, Alberto Armigliato, Gianluca Pagnoni and Filippo Zaniboni

Dipartimento di Fisica

Università di Bologna

Viale Carlo Berti Pichat, 8-40127 Bologna, Italy

ABSTRACT

Scenarios represent a very useful technique for the definition and evaluation of tsunami hazard and risk for any given region, and a basic step in the frame of tsunami mitigation and preparedness and of sustainable coastal zone development. With the exception of very few countries, like Japan and the United States, emergency plans in the rest of the world have never taken serious care of tsunamis until the occurrence of the giant Indian Ocean tsunami on December 26, 2004. That event dramatically brought the problem of tsunami hazard and risk assessment to the general attention and showed the urgent need for implementation of tsunami early warning systems (TEWSs). The problem is particularly urgent for the Mediterranean countries that are known to have been attacked by numerous tsunamis in the past, several of which had catastrophic size and impact. This paper is an attempt to develop some simple scenarios of earthquake-generated tsunamis in the Mediterranean. We identify four different seismogenic areas in the western, central and eastern sectors of the basin. For each of them, we take into account a seismic fault capable of generating an earthquake with magnitude equal or larger than the highest magnitude registered in that region in historical times. Then we simulate numerically the ensuing tsunamis, highlighting the basic features of the wave propagation and roughly identifying the coastal sectors that are expected to suffer the heaviest tsunami effects. One of the most important outcomes is that these scenario tsunamis attack the nearest coasts within at most 15 minutes, which poses serious constraints for designing appropriate TEWS for the Mediterranean.

KEYWORDS: Large Tsunamigenic Earthquakes, Mediterranean Region, Tsunami Modelling, Tsunami Propagation, Tsunami Travel Times

INTRODUCTION

The recent catastrophic giant tsunami that was generated by the December 26, 2004 earthquake offshore western Sumatra has raised a number of urgent issues regarding tsunamis. In particular, the Indian Ocean event pointed out dramatically that we have very little knowledge on mega-tsunamis and on their potential impact on human habitat, and also that the international community lacks a clear strategy of how to deal with these mega-events. This holds also for the countries facing the Mediterranean Sea. It is perfectly known from tsunami catalogues that the Mediterranean Sea coasts were attacked by several tsunamis in the past, and that many of them had catastrophic size and impact. These catalogues, which are largely incomplete as regards the early history, tell us that tsunamis in the Mediterranean, like in the rest of the world, are mostly due to earthquakes, landslides, rockfalls, and volcanic activity. It must be stressed that many tsunami sources are located close to densely populated areas. Moreover, many known occurrences of tsunamis are still not linked to reliable sources, which is partly due to the fact that the zoning of tsunamigenic sources is incomplete as regards offshore faulting and submarine landslides. All the previous considerations clearly indicate that tsunami hazard and risk assessment for Mediterranean countries is an urgent need that should be carried out both at local and at regional scales. In this paper we concentrate on the use of scenarios to study some basic features of tsunami propagation in the Mediterranean region. We limit our attention to tsunamis generated by earthquakes. Based on the historical records contained in the available tsunami catalogues as well as on basic seismotectonic information, we concentrate on four main source regions. One of them is located in the western portion of the Mediterranean, in correspondence with the Algeria coastal belt. The second source region coincides with the Hyblaean-Malta escarpment, a huge topographic structure found off eastern Sicily, Italy. Finally, we take into account two different thrust faults found in eastern Mediterranean: one coincides with the

western sector of the Hellenic trench, while the second lies at the eastern end of the Hellenic trench itself, in front of the south-western Turkish coast.

BACKGROUND

1. Tectonics

The Mediterranean area is characterised by very complex tectonics that can be generally described in the frame of the collision between the Eurasian and African plates. A detailed description of the tectonic processes taking place in the region is beyond the scope of this paper, and the interested reader can refer to numerous studies published in the scientific literature in the last decade (see, e.g., McClusky et al., 2000; Mantovani et al., 2001; Di Luccio et al., 2003; Henares et al., 2003; Marone et al., 2003; Carminati and Doglioni, 2004; Marone et al., 2004; Goes et al., 2004; Papazachos et al., 2006, and references therein). Here we will briefly describe the main tectonic structures, with special emphasis on three different regions that will be adopted as seismogenic-tsunamigenic sources in our numerical simulations.

The Eurasia-Africa plate boundary collision assumes different expressions in different portions of the Mediterranean Sea which we summarise with the aid of Figure 1(a). In western Mediterranean, the convergence between the two plates is responsible for the Betics Cordillera in southern Spain and the Maghrebides mountain belt in northern Africa. In central Mediterranean, several structures with complex mutual interactions can be recognised: the slowly converging orogenic belts of the Alps-Dinarides and of the Apennines, the rapidly extending Tyrrhenian basin, huge subduction margins such as the Calabrian Arc, the southern Italy volcanism and the very steep Hyblaean-Malta escarpment. Similar complexity is evident also in eastern Mediterranean. The African plate subducts underneath Eurasia along the Hellenic Arc at a rate of about 1 cm/year, while the Aegean Sea represents an extensional basin with opening rates in the order of 3.5-4 cm/year (McClusky et al., 2000). The Cyprean Arc is the expression of the collision between the Africa plate and the Anatolia microplate. Moreover, the Mediterranean Ridge, found south-west of the Hellenic trench, represents a structure whose nature is still highly debated (see Le Pichon et al., 2002). Finally, the North-Anatolian Fault is a dextral system of faults forming the broad boundary between the Eurasian plate and the Anatolian block.

2. Seismicity and Tsunami Activity

Seismicity in the Mediterranean basin is strongly connected to the tectonic features outlined above. Figure 1(b) shows the epicentral locations contained in the USGS National Earthquake Information Center catalogue (USGS/NEIC, <http://neic.usgs.gov/neis/epic/>) since 1973. Only the earthquakes with magnitude greater than 4 are plotted. Furthermore, only shallow (depth ≤ 30 km) earthquakes are plotted, since the tsunamigenic potential of deeper events can be neglected.

Since tsunamis in the Mediterranean, as well as in other parts of the world, are mostly generated by earthquakes, it is no surprise that the geographical distribution of the historical tsunamis in the region generally resembles the trend of seismicity. Figure 1(c) shows the tsunami events listed in the European Tsunami Catalogue by Tinti et al. (2001a), which is an updated version of the tsunami catalogue compiled in the framework of the European Union Projects GITEC (Genesis and Impact of Tsunamis on the European Coasts) and GITEC-TWO (Genesis and Impact of Tsunamis on the European Coasts – Tsunami Warning and Observations) (see Tinti et al., 1999). The catalogue spans the time interval 6000 B.C. – 2003 A.D.; the original catalogue has been updated here with the Stromboli island tsunamis of December 30, 2002, and with the North Algeria tsunamis of May 21, 2003. Events are plotted with symbols of different sizes, which are proportional to the tsunami intensity measured on the Sieberg-Ambraseys scale (Ambraseys, 1962). We observe that the catalogue does not include events generated in the Levantine Sea, in eastern Mediterranean.

SUB-REGIONS AND SELECTION OF SEISMIC SOURCES

Based both on seismicity and on tsunami distribution, we will concentrate on three different sub-regions: north-Algeria (western Mediterranean), southern Tyrrhenian and eastern Sicily (central Mediterranean), and the Hellenic Arc (eastern Mediterranean). The three panels of Figure 2 offer a closer look at the recent deformation styles characterizing the three sub-regions. The plotted focal mechanism have been extracted from the database of Earthquake Mechanisms of the Mediterranean Area (EMMA

version 2.2) (Vannucci and Gasperini, 2004). Since we are mainly interested in the tsunamigenic potential of the earthquake sources, only events with hypocentral depths shallower than 30 km have been plotted. For each sub-region, we will briefly describe the most significant recorded earthquakes and tsunamis, summarise the available information on the possible tsunamigenic seismic sources, and take these as the basis to develop a scenario for the propagation of the tsunami from the source throughout the entire Mediterranean basin.

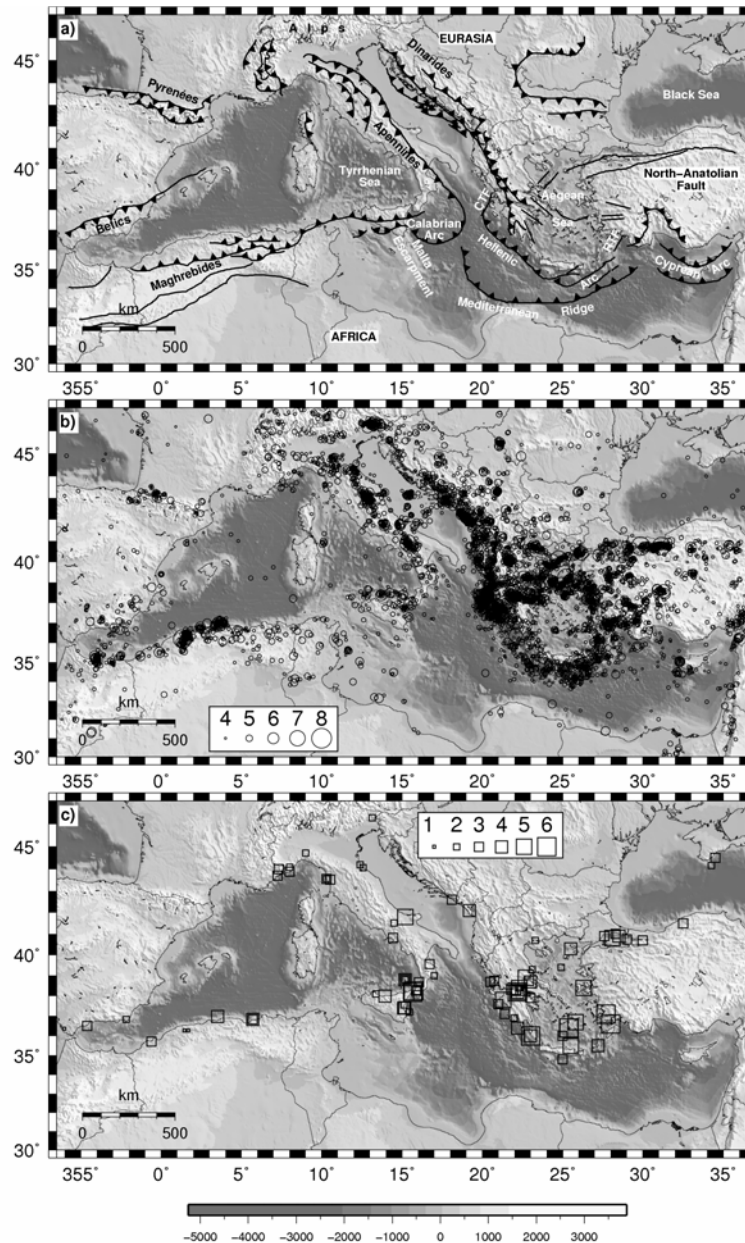


Fig. 1 Geographical sketch of the Mediterranean area, with shaded topography and bathymetry: (a) major tectonic lineaments (redrawn after Faccenna et al., 2003; Papazachos et al., 2006) (lines with triangles indicate subduction margins; CTF and RTF stand respectively for the right-lateral Cephalonia Transform Fault and for the left-lateral Rhodes Transform Fault); (b) outline of the seismicity in the area as reported in the USGS National Earthquake Information Center catalogue since 1973 (only the earthquakes with magnitude greater than 4 and depth shallower than 30 km are plotted, and the symbol size is proportional to the magnitude); (c) tsunami activity deducible from the European catalogue of tsunamis (Tinti et al., 1999; Tinti et al., 2001a) (size of the symbols used to plot the events is proportional to the tsunami intensity, measured on the Sieberg-Ambraseys 6-degree scale (Ambraseys, 1962))

1. Algeria

Recent studies concerning historical and instrumental seismicity (e.g., Harbi et al., 2003a, 2003b) indicate that northern Algeria is exposed to relevant seismic hazard and risk. Several large earthquakes occurred in this region in historical times. The largest recorded event is the El Asnam earthquake that occurred on October 10, 1980. It was characterised by magnitude $M_S = 7.3$ and macroseismic intensity $I = X$ in the MKS scale. According to the USGS catalogue, the earthquake claimed the lives of more than 5000 people (http://neic.usgs.gov/neis/eqlists/sig_1980.html). The last destructive seismic event occurred on May 21, 2003. This earthquake had magnitude $M_W = 6.8-6.9$ and was located at (3.65°E, 36.83°N), about 40 km east of Algiers, with hypocentral depth in the order of 8-10 km (Bounif et al., 2004). More than 2000 people were killed, 11,000 injured and 200,000 became homeless (Yelles et al., 2004). The earthquake generated a tsunami that was observed in Algeria and Spain and was recorded by the tide gauges in as far as Nice, France, and Genoa, Italy (see Hebert and Alasset, 2003 for details). Several papers have been published recently dealing with the retrieval of the parent fault parameters based on different data and analysis techniques (Bouhadad et al., 2004; Bounif et al., 2004; Braunmiller and Bernardi, 2005; Delouis et al., 2004; Déverchère et al., 2005; Meghraoui et al., 2004; Semmane et al., 2005; Yelles et al., 2004). Moreover, numerical simulations of the tsunami can be found in Hebert and Alasset (2003). The general conclusion that can be deduced from these studies is that the earthquake was generated by a thrust fault, dipping at about 40°-50° towards south-east, with relevant extension offshore the Algerian coasts, hence producing a significant deformation of the seafloor that was responsible for the tsunami generation.

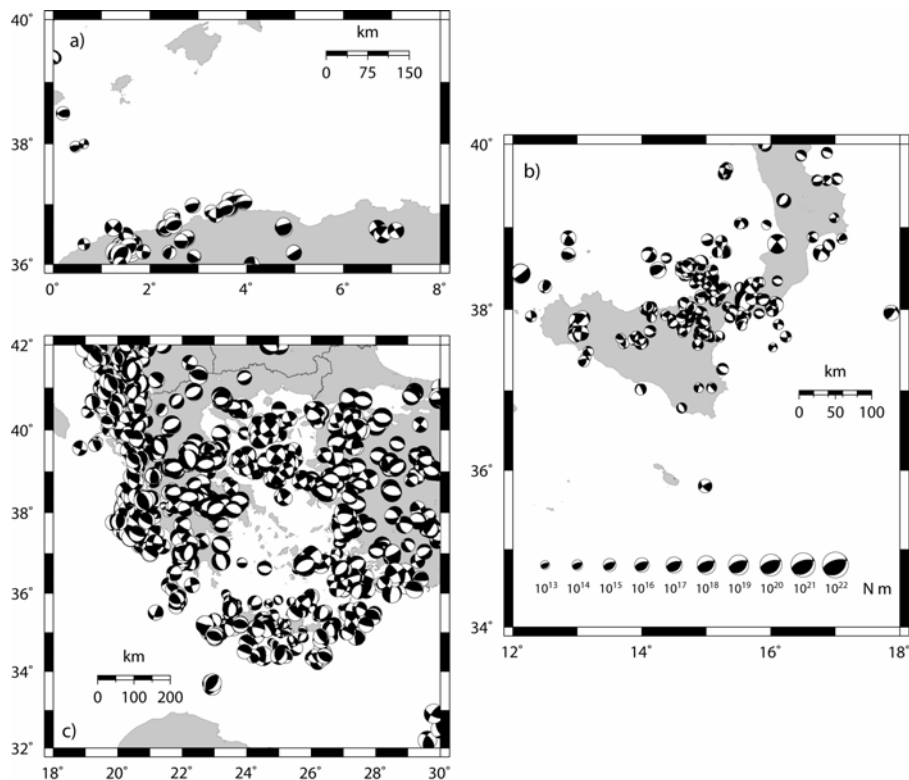


Fig. 2 Focal mechanisms for the shallow seismicity (hypocentral depth less than 30 km) deduced from the EMMA catalogue (version 2.2) for the three sub-regions examined in this paper: (a) northern Algeria (western Mediterranean); (b) southern Tyrrhenian and eastern Sicily (central Mediterranean); (c) Hellenic Arc (eastern Mediterranean)

In the earthquake scenario we examine in this paper, the source of the May 21, 2003 earthquake and the associated tsunami has been adopted as the central portion of a three-segment hypothetical structure, resulting from a westward and eastward 40-km length prolongation of the original fault. The strike directions of the prolongations mimic the local shape of the coastal belt (see Table 1). The resulting source is characterised by $M_W = 7.6$ and scalar seismic moment $M_0 = 2.8 \times 10^{20}$ N · m.

Table 1: Fault Parameters for the Three-Segment Hypothetical Algeria Source Considered in This Study

	Western Segment	Central Segment	Eastern Segment
L (km)	40	64	40
W (km)	32	32	32
Strike (degree)	84	54	94
Dip (degree)	47	47	47
Rake (degree)	88	88	88
Slip (m)	2	2	2
Depth (m)	1000	1000	1000
The depth reported in the last row refers to the upper border of the rectangular fault segments. The corresponding approximate values of the magnitude M_w and of the seismic moment M_0 are respectively 7.6 and 2.8×10^{20} N·m.			

2. Southern Tyrrhenian – Eastern Sicily

The southern Tyrrhenian basin and eastern Sicily are, without doubt, among the most active regions of the entire Mediterranean. Italian earthquake catalogues (e.g., CPTI04¹) contain numerous events with magnitude exceeding 7 in this region, and tsunami catalogues (e.g., Tinti et al., 2004) indicate that the most devastating Italian tsunamis took place here. As examples, it will be sufficient to recall the tsunamis generated by the earthquakes of January 11, 1693 and of December 28, 1908, hitting eastern Sicily and the Messina Straits; in both cases, tsunami waves locally exceeding 10 meters were observed, and the total number of victims caused by the earthquake and the tsunami was in the order of several tens of thousands.

In this study, we will take the event of January 11, 1693 as a starting point to develop our tsunami scenario. According to CPTI04¹, the parent earthquake was the highest magnitude event ($M \sim 7.4$) in the Italian seismic history. An area of about 14,000 km² suffered almost complete destruction, and the major towns of Catania, Augusta, Noto and Siracusa, as well as a number of smaller centres and villages, were razed to the ground. The earthquake generated a tsunami that devastated the entire eastern Sicily coasts, damaged the Malta archipelago and was observed in a large portion of the western Ionian Sea. There is still a debate in the scientific community on the location of the earthquake fault and on the tsunami generating cause. Based mainly on macroseismic studies, some authors (e.g., Sirovich and Pettenati, 2001; DISS_3²) identify a fault with predominant transcurrent mechanism located in the eastern Sicily mainland. Other studies, based on offshore seismic data analysis and morpho-tectonics arguments (e.g., Bianca et al., 1999; Argnani and Bonazzi, 2002, 2005), or on tsunami numerical simulations (Tinti et al., 2001b; Tinti and Armigliato, 2003), propose that the parent fault should be found off eastern Sicily, in correspondence with the huge topographic structure known as Malta escarpment, characterised by active extensional tectonics. No widely agreed solution exists to date, and other sources cannot be excluded a priori, both for the earthquake and for the tsunami. For example, as regards the tsunami, the hypothesis that some local offshore mass movements, possibly triggered by the earthquake, could have contributed to the tsunami generation cannot be ruled out. Anyhow, there are two main points that, in our opinion, are in favour of the Malta-escarpment-offshore earthquake source being mainly responsible for the tsunami. First, the faults along the Malta escarpment are very well characterised from the geological point of view and there are evidences for their recent activity, at least in the part lying north of Siracusa (Argnani and Bonazzi, 2005). No geological evidence exists instead for the onshore faults, which are mainly the results of macroseismic data inversion. Secondly, the seismic origin of the tsunami seems to be favoured by the very large extension of the severely affected coastal areas. It is well known that earthquake-generated tsunamis are usually observed on a regional scale, while landslide-generated tsunamis tend to have a more local character. Hence, if we invoke the possibility of an offshore landslide being the only possible cause for the 1693 tsunami, we must take into account a huge-volume source (possibly larger than several tens of millions of m³). But, to date, no geological evidence exists in this respect. A more realistic hypothesis

¹ Catalogo Parametrico Dei Terremoti Italiani, 2004 version (in Italian); available at <http://emidius.mi.ingv.it/CPTI/>

² Database of Individual Seismogenic Sources: Version 3; available at <http://www.ingv.it/~wwwpaleo/DISS3/>

is that the earthquake could have triggered moderate-size landslide, whose effect could have been that of modulating locally the tsunami effects. But at the moment these represent purely theoretical speculations.

Owing to the above considerations, we will adopt here the hypothesis of a tsunami source lying offshore along the Malta escarpment. In order to consider a worst-case scenario, we consider a single fault running parallel to the Malta escarpment for a length of 84 km and capable of generating an earthquake with magnitude $M_w = 7.4$, coinciding with the value reported in CPTI04¹. The relevant fault parameters are listed in Table 2.

Table 2: Fault Parameters for the Hypothetical Normal Fault along the Malta Escarpment, Offshore Eastern Sicily

L (km)	84
W (km)	23
Strike (degree)	342
Dip (degree)	30
Rake (degree)	270
Slip (m)	2
Depth (m)	1000
The corresponding approximate values of the magnitude M_w and of the seismic moment M_0 are respectively 7.4 and 1.4×10^{20} N·m.	

3. Hellenic Arc

Together with Italy and Turkey, Greece is characterised by the highest tectonic activity in the Mediterranean. Due to its very ancient civilization, its historical record of earthquakes and tsunamis is among the longest in the world. Greece is characterised by a very complicated tectonic setting, dominated by the subduction of the African lithosphere beneath the Eurasian plate along the Hellenic Arc, consisting of an outer sedimentary arc and an inner volcanic arc (see, among the others, Benetatos et al., 2004; Laigle et al., 2004; Papazachos et al., 1999, 2000a, 2006; and references therein). The Hellenic Arc is bounded at its north-western and eastern ends by two major transform faults, known as the Cephalonia (right-lateral) and the Rhodes (left-lateral) transform faults (respectively CFT and RTF in Figure 1(a)). The subduction is accompanied by a prominent shallow seismicity with low-angle thrust faults along the Hellenic arc, normal faulting in the back-arc Aegean area, and intermediate depth seismicity forming a well-defined Benioff zone in the southern Aegean. The highest magnitude reported in earthquake catalogues for Greece (e.g., Papazachos et al., 2000b) is 8.3, and refers to the July 21, 365 earthquake (e.g., Papazachos, 1996; Stiros, 2001; Stiros and Papageorgiou, 2001). The hypocentre of this earthquake was probably located offshore western Crete, along a major thrust fault parallel to the western Hellenic trench. The earthquake generated a huge tsunami that was very likely destructive along the western Crete coast and is known to have destroyed the Nile delta area in Egypt (see Stiros, 2001; Stiros and Papageorgiou, 2001; Dominey-Howes, 2002; Papadopoulos, 2002). Another important example of tsunami observed in large portions of the eastern Mediterranean and generated by an earthquake source in the broad Hellenic arc area is represented by the 1303 event. The estimated magnitude for the earthquake is 8 (Papazachos, 1996). According to historical sources (e.g., Guidoboni and Comastri, 1997), severe tsunami effects were experienced at least along south-eastern Crete, southern Rhodes, western Cyprus, southern Syria and northern Israel, and finally the Nile delta region in Egypt.

Though it is known that large tsunamis in Greece may be related also to volcanic activity (see the giant Thera volcano explosion tsunami that occurred about 3500 years ago and is believed to have undermined the Minoan civilization (McKoy and Heiken, 2000; Minoura et al., 2000)), in the present study we focus on tsunamigenic earthquake sources and take into account two distinct sources along and at the eastern end of the Hellenic trench. The first is a two-segment source running parallel to the western section of the trench and mimicking the source that was very likely responsible for the 365 A.D., $M = 8.3$ earthquake and tsunami. Its focal parameters are listed in Table 3. The second is a large thrust fault lying offshore the south-western Turkish coast, whose parameters are listed in Table 4. Following some authors (e.g., Papazachos, 1996), this fault could be responsible for the 1303 huge tsunami, although very

different hypotheses exist on the epicentral position of the parent earthquake (e.g., Guidoboni and Comastri, 1997; El-Sayed et al., 2000).

Table 3: Fault Parameters for the Hypothetical Two-Segment Thrust Fault along the Western Hellenic Arc

	Northern Segment	Southern Segment
L (km)	206	233
W (km)	38	38
Strike (degree)	326	312
Dip (degree)	20	20
Rake (degree)	90	90
Slip (m)	10	10
Depth (m)	1000	1000
The corresponding approximate values of the magnitude M_w and of the seismic moment M_0 are respectively 8.3 and 3.2×10^{21} N·m		

Table 4: Fault Parameters for the Hypothetical Thrust Fault along the Eastern Hellenic Arc

L (km)	190
W (km)	35
Strike (degree)	300
Dip (degree)	20
Rake (degree)	90
Slip (m)	5
Depth (m)	1000
The corresponding approximate values of the magnitude M_w and of the seismic moment M_0 are respectively 8.0 and 1.1×10^{21} N·m.	

NUMERICAL MODELING OF EARTHQUAKE-INDUCED TSUNAMIS

The propagation of the tsunami is computed by means of a finite-element (FE) model solving the non-linear shallow water equations. This model has been developed specifically for tsunami analysis by the University of Bologna, Italy (see Tinti et al., 1994). The code has been extensively used to study near-field propagation of tsunamis generated by near-shore earthquakes (see, for example, Tinti et al., 2001b; Piatanesi and Tinti, 2002; Tinti and Armigliato, 2003). The FE code makes use of meshes consisting of triangular elements that are created through a mesh building code that tends to produce triangles with the highest index of isotropy (typically equilateral) and a uniform crossing time (Tinti and Bortolucci, 1999). The numerical scheme assumes null initial velocity and the initial shape of the sea-free surface to be coincident with the vertical coseismic deformation of the ocean bottom. The latter is computed, given the fault parameters of Tables 1-4, by means of Okada's formulas (e.g., Okada, 1992) corrected in order to account for the sea bottom bathymetry, according to the method first introduced by Tanioka and Satake (1996) and then adapted by Tinti and Armigliato (1999) to FE schemes.

The boundary conditions consist of full wave transmission on the open boundaries (open sea), and pure wave reflection on the coastal boundaries that are treated as vertical walls. Technically, this means that the tsunami model does not compute run-up heights, but only maximum water elevations at the vertical coast. However, this is not a significant limitation for the purpose of this paper, since (1) maximum water elevations are known to be a reasonable approximation of run-up heights for most coastal morphologies (see e.g., Synolakis, 1991), and (2) in this study we are interested in the general features of the tsunami wave propagation in the Mediterranean basin rather than in the detailed analysis of the tsunami impact along the coasts.

RESULTS AND DISCUSSION

1. Algerian Earthquake Scenario

The initial tsunami condition computed on the basis of the fault parameters listed in Table 1 is plotted in Figure 3(a). Unlike the other scenarios which we will examine later, in the case of the Algerian scenario the earthquake source is not completely placed offshore, with the consequence that only part of the coseismic deformation affects the sea bottom and is available for tsunami generation. The initial displacement field is characterised by uplift (sea water rise) close to the coast and by a smaller downlift (sea retreat) offshore. The maximum uplift is 1.25 m, while the maximum downlift is -0.31 m.

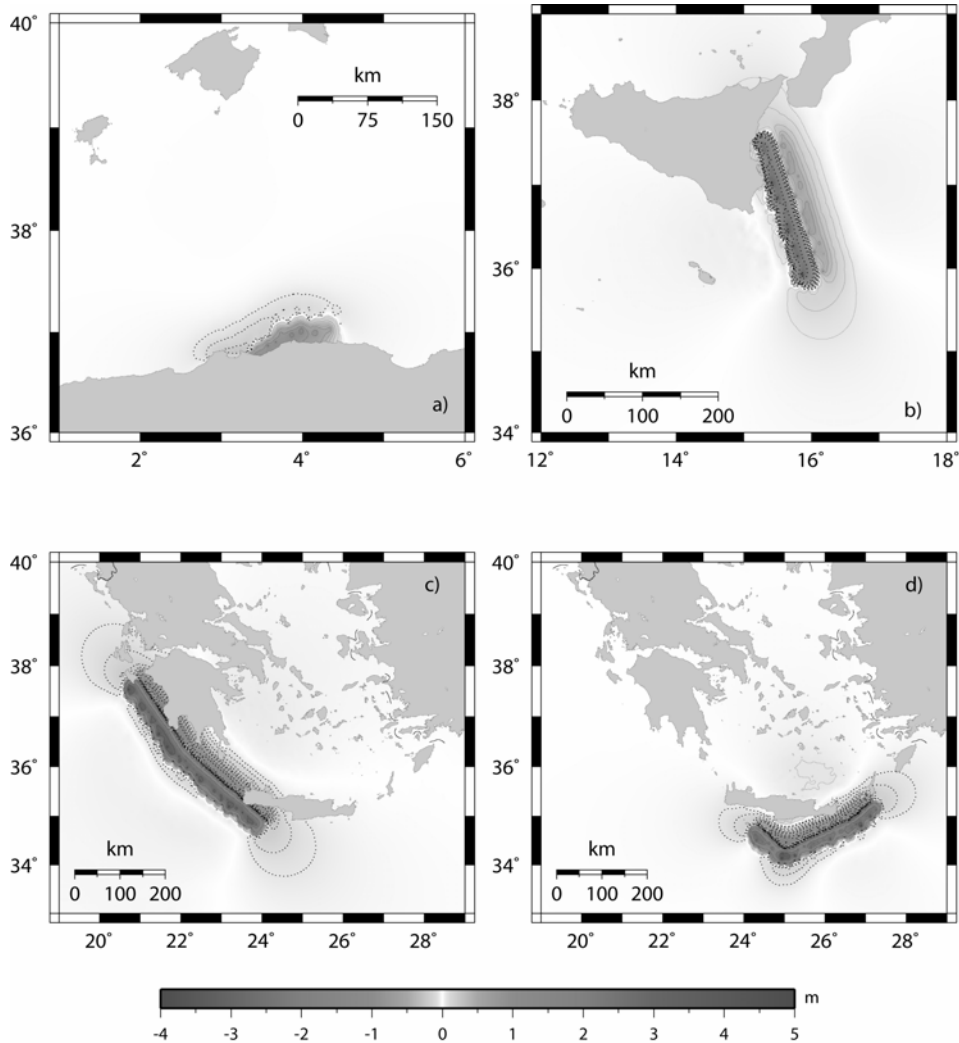


Fig. 3 Initial tsunami conditions (coinciding with the vertical coseismic displacement of the seafloor) for each of the four hypothetical earthquake sources considered in this study (the irregular shape of the fields is due to the effect of the local bathymetry; solid and dotted contours indicate positive and negative sea-water elevations, respectively)

Figure 4 shows four snapshots of the tsunami propagation, taken at 15-minute intervals after the tsunami onset. It is relevant to observe that after only 15 minutes, the tsunami has attacked a long portion of the nearest coastal segment in Algeria. After 30 minutes, the tsunami waves attack the Balearic Islands to the north and, due to basin morphology, the leading tsunami fronts begin to elongate roughly in a North East-South West direction. The south-eastern coasts of Spain, and in particular the Costa Blanca, experience the tsunami arrival after 45 minutes; at the same time, the tsunami has hit the entire Balearic archipelago and has reached the south-western coasts of Sardinia. Furthermore, almost the entire Algerian coastline has been attacked by the tsunami waves. Our final snapshot is taken one hour after the earthquake: tsunami waves enter the Alboran Sea to the south-west and strike the whole western Spanish

coastal belt; along North Africa, the Moroccan and Tunisian coasts are attacked; and to the north, tsunami waves are close to reaching the south-eastern French coasts (Côte d'Azur).

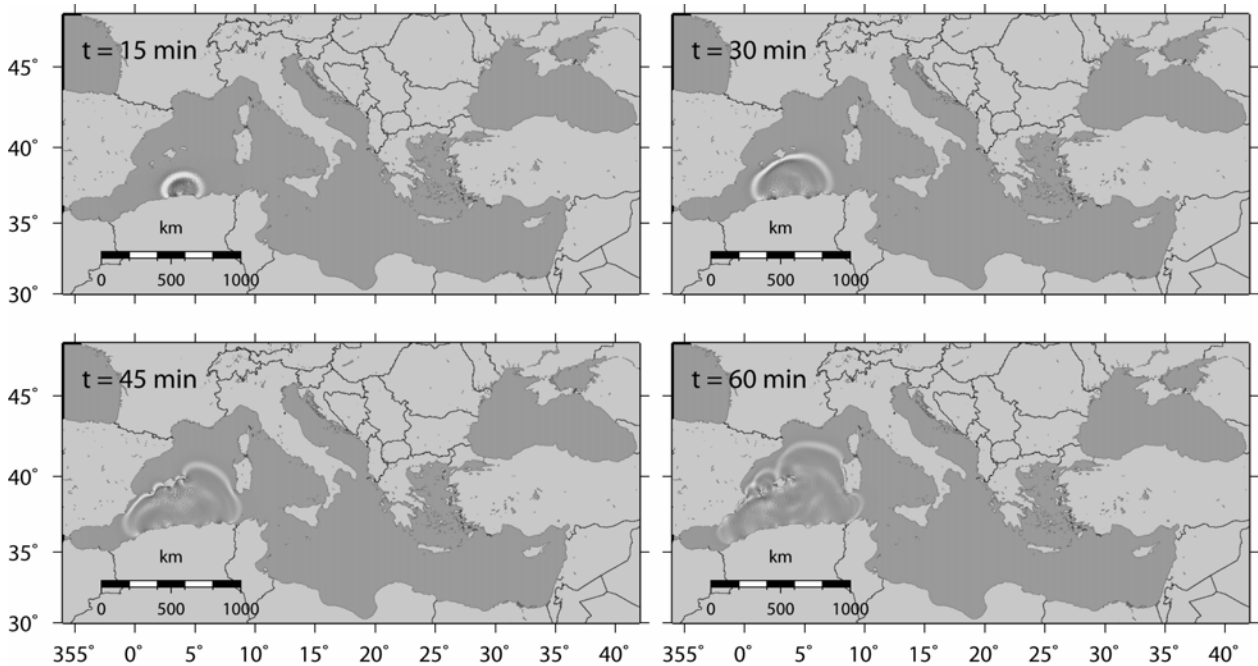


Fig. 4 Tsunami scenario related to the hypothetical Algeria Earthquake fault (snapshots of the computed water elevation fields are at 15-minute intervals after the earthquake)

Figure 5 shows the maximum positive and negative tsunami heights computed in the Mediterranean basin. The fields can be interpreted roughly as an image of the tsunami energy propagation. The resolution of our FE grid does not allow to predict correctly the values of the extreme water elevations, which are expected to be underestimated by our simulations. However, we can still draw reliable conclusions about which stretches of the Mediterranean coastline are expected to experience the most severe tsunami effects. First, there appears to exist a clear preferential direction of energy propagation from the source region in North Algeria towards the Balearic Islands. This is in agreement with what is known of the May 21, 2003 tsunami, whose strongest effects were observed in Majorca and Minorca islands, with water waves as high as 2 m (Hebert and Alasset, 2003). Furthermore, our simulations predict that the Spanish stretch of coast called Costa Blanca should experience non-negligible tsunami effects. Tsunami waves are expected to attack with smaller waves almost the entire north-African shoreline, the western coasts of Spain, the Ligurian sea coasts as well as western Sardinia and Corsica. Notice further that tsunami height is negligible inside the Tyrrhenian sea and east of the Malta escarpment. Concerning maximum elevations expected along the French and Ligurian coasts, our results are in agreement with the scenario that Pelinovsky et al. (2002) developed and discussed starting from a $M = 6.8$ earthquake located offshore western Algeria, approximately in correspondence with the source area of the 1954 event.

2. Eastern Sicily Scenario

The tsunami initial condition for this $M_w = 7.4$ scenario is plotted in Figure 3(b). The source we are considering is a normal fault, placed completely offshore and parallel to the Malta escarpment, which induces a sea bottom deformation characterised by a subsidence in front of the eastern Sicily coasts and a smaller uplift in the open Ionian sea. Maximum negative and positive vertical deformations are -1.0 m and 0.2 m, respectively.

The tsunami propagation simulated by our model is illustrated in the four snapshots of Figure 6. The tsunami field plotted at 15 minutes after the tsunami generation exhibits an elongated shape in the North West-South East direction, which is imputable to the earthquake source orientation. It is important to observe that all eastern Sicily, together with southern Calabria, are affected by the tsunami within such a short period of time. After 30 minutes, the tsunami propagation is clearly seen to depend heavily on the bathymetry. Propagation is slow in westward direction due to the shallow waters of the Sicily channel and

of the Tunisia-North West Libya basin. Conversely, tsunami waves travel much faster southward parallel to the Malta escarpment heading for the Sidra Gulf, and north-eastward in direction of the Greek coasts. After 45 minutes almost the entire Ionian Calabria coast is hit. The last snapshot after one hour shows that the region already attacked by the tsunami includes southern Italy, Malta, southern Albania, western Greece, southern Peloponnesus. Moreover, tsunami waves are very close to attacking western Crete and north-eastern Libya.

The maximum and minimum tsunami elevations are displayed in Figure 7. Tsunami energy is clearly seen to channel preferentially along a South West-North East direction going from Tunisia to Albania and Greece. The most severely affected regions are the Ionian coasts of Italy (eastern Sicily, Ionian Calabria, Basilicata and southern Apulia), Malta, southern Albania and western Greece (especially the Ionian Islands), and finally the Tunisian coasts, with most intense tsunami effects expected in the Gabes Gulf. Note that some tsunami effects are also expected in the southern Adriatic Sea, the Sidra gulf in Libya, the Egyptian coasts, and some limited coastal zones in the eastern Mediterranean basin. We observe further that no significant tsunami propagation is predicted by our model for the Tyrrhenian Sea and the western Mediterranean.

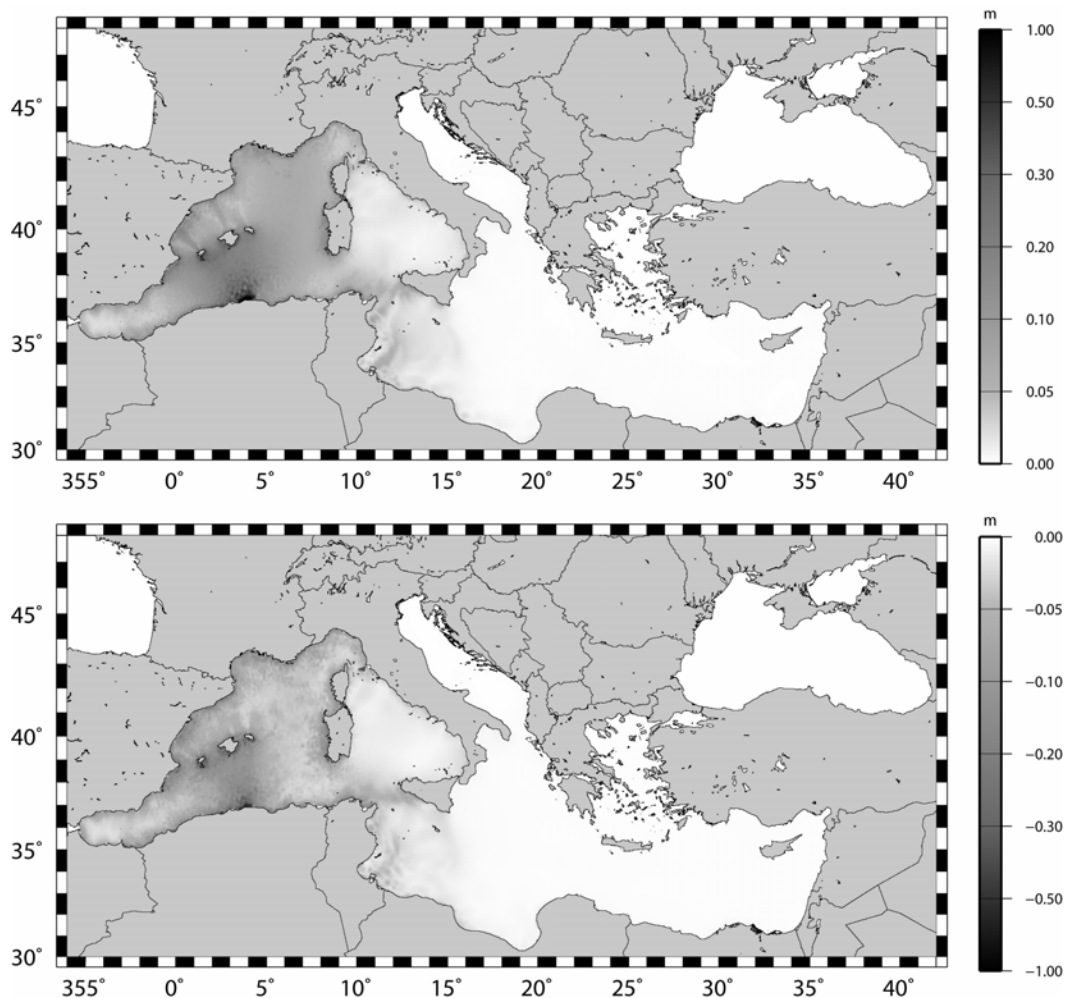


Fig. 5 Maximum positive (upper panel) and negative (lower panel) tsunami wave heights computed for the Algerian source scenario

3. Western Hellenic Arc Scenario

We take in consideration first an $M_w = 8.3$ earthquake generated on a two-segment thrust fault running parallel to the western Hellenic trench from northern Peloponnesus to western Crete. The tsunami initial condition for this first case is plotted in Figure 3(c). The maximum positive and negative initial water elevations are 4.9 m and -1.6 m, respectively.

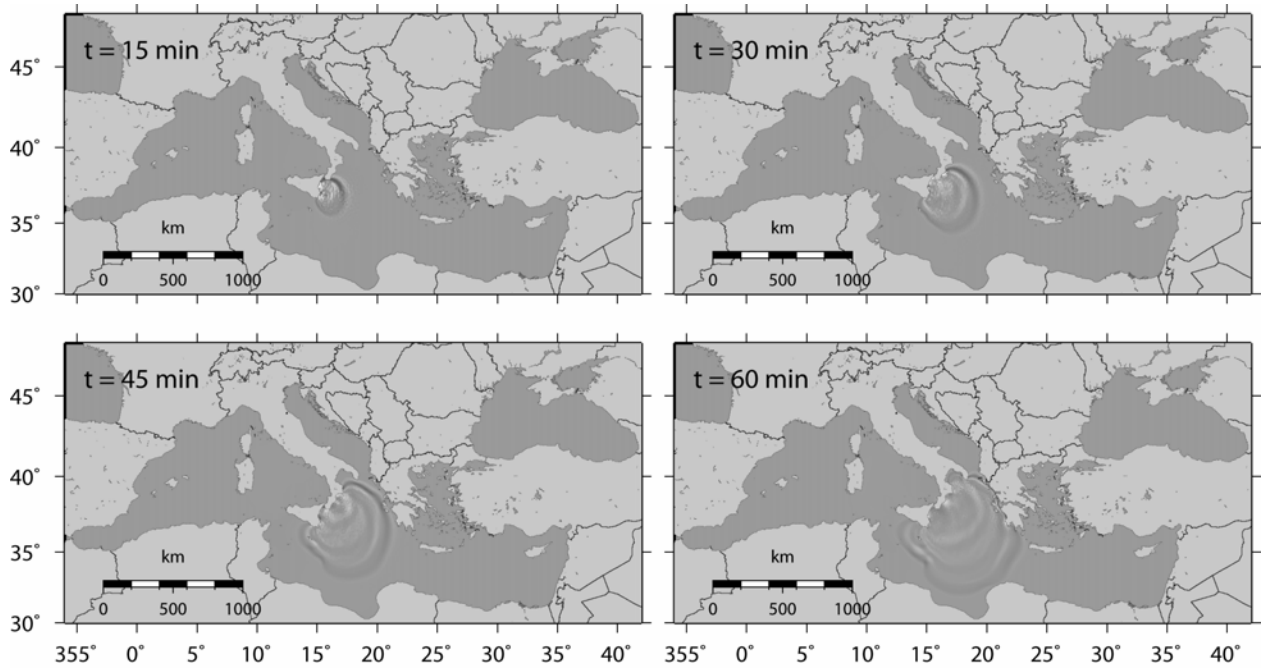


Fig. 6 Snapshots of the tsunami elevation fields computed for the eastern Sicily scenario

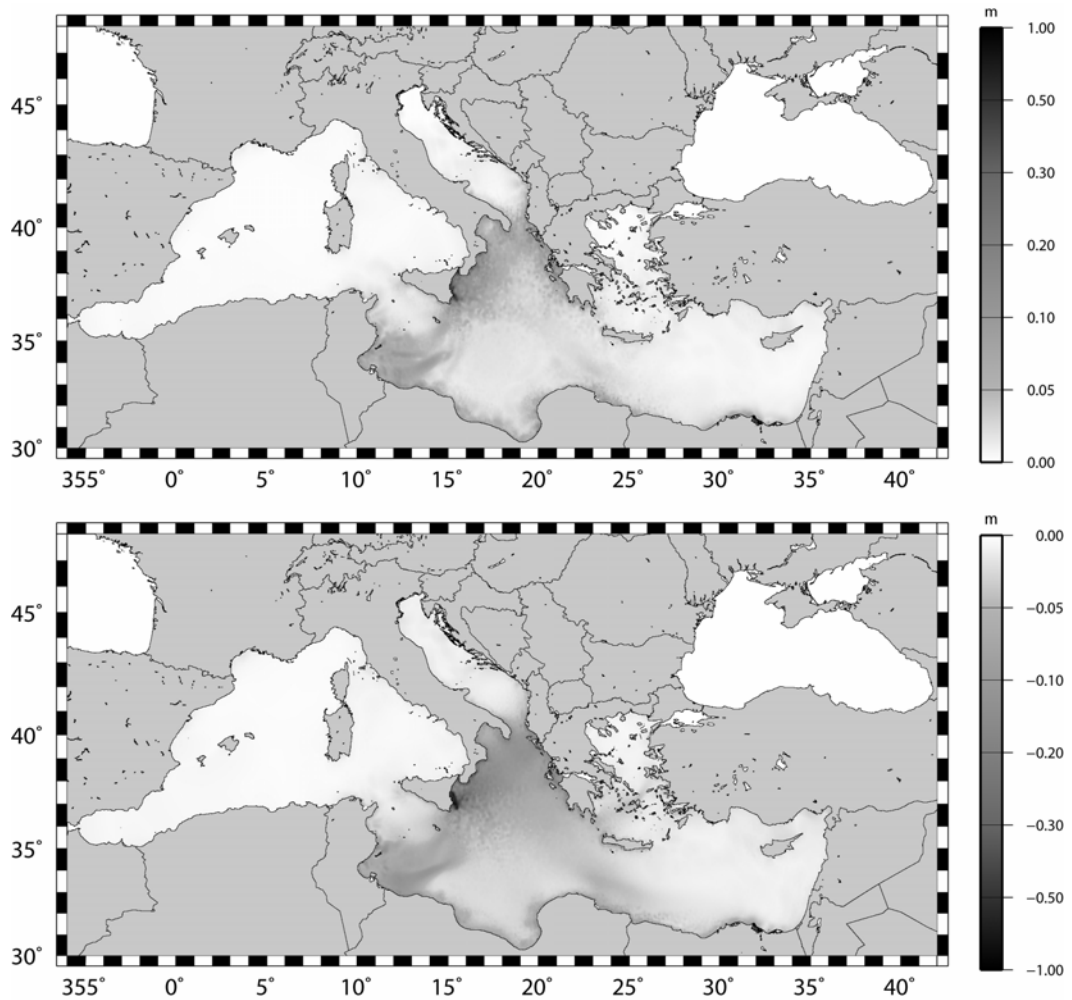


Fig. 7 Extreme water elevation fields computed for the eastern Sicily scenario

The ensuing tsunami propagation features can be commented with the aid of Figure 8. In the image showing the tsunami field computed 15 minutes after the tsunami initiation, we observe that all Ionian Greece coasts, the entire West Crete and almost all South Crete is already affected by the tsunami, and that a strong positive leading front is travelling in south-west direction towards the Libyan sea. Thirty minutes after the earthquake, the leading front has inundated North-East Libya, the largest part of Crete and the South-West Aegean islands. Furthermore, the tsunami propagates north-west towards southern Italy and south-east towards Egypt with a characteristic sequence of two successive crests. The image describing the tsunami propagation after 45 minutes indicates that waves have already attacked southern Apulia and Calabria, are approaching eastern Sicily, and are slowly propagating inside the Aegean Sea, with a pattern that is strongly influenced by the very complex morphology. One hour after the tsunami has violently attacked eastern Sicily to the west, it is approaching with smaller but still relevant energy towards Egypt and south-eastern Turkey, and continues its propagation towards the central portion of Libya and the Sidra Gulf to the south, and towards Tunisia to the west.

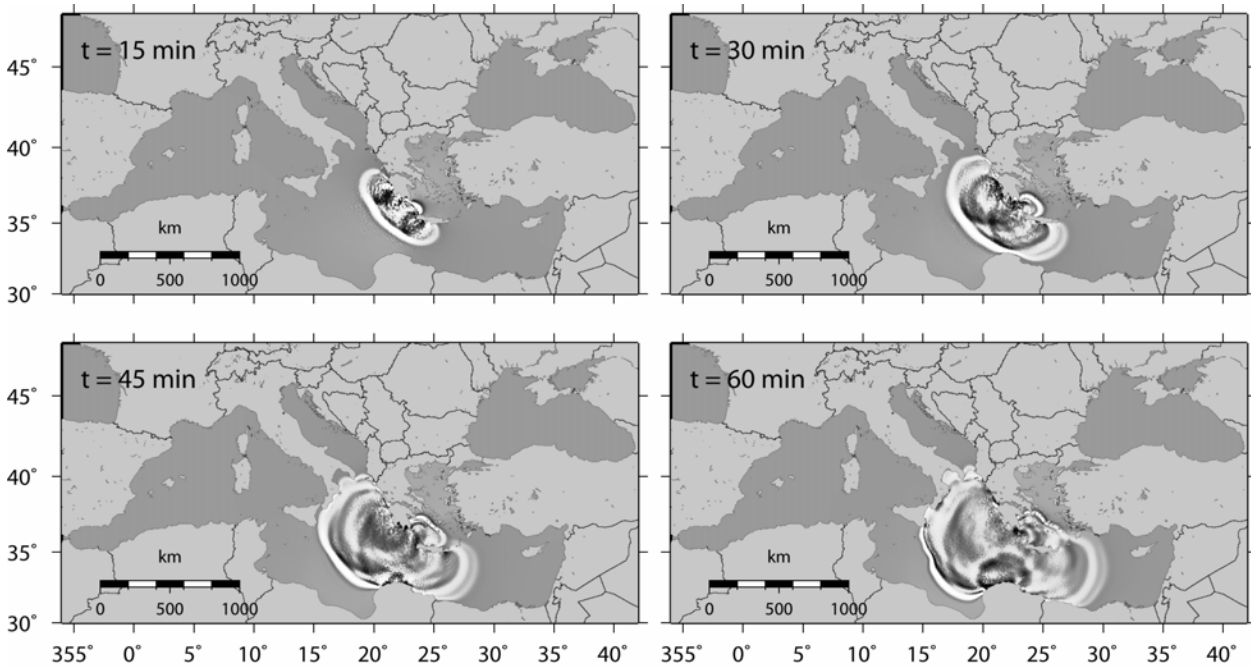


Fig. 8 Snapshots of the tsunami elevation fields computed for the western Hellenic Arc scenario

The extreme water elevation fields shown in Figure 9 indicate that, as in the previous cases, the geometry of the source strongly influences the preferential direction of tsunami energy propagation. The strongest tsunami effects are predicted to occur all along western Greece, Crete, on the south-western Aegean Sea, as well as along West Tunisia (Gabes Gulf), the entire Libyan coast, and West Egypt. Finally, some tsunami energy is seen to propagate inside the Adriatic Sea, while no relevant tsunami effects are expected for the western Mediterranean.

4. Eastern Hellenic Arc Scenario

Our last scenario is regarding a thrust source located at the eastern end of the Hellenic Arc, striking at about 300° in front of the south-western Turkish coast. The source, whose parameters are listed in Table 4, is characterised by a magnitude $M_w = 8.0$ and induces maximum positive and negative vertical sea bottom deformations of 1.9 m and -0.7 m, respectively. The complete initial tsunami condition is displayed in Figure 3(d).

Figures 10 and 11 describe the basic characteristics of the tsunami propagation. The same general considerations made in the previous cases also hold for this scenario, so we will not go into further details. It will be sufficient to stress that, in about 1 hour, the whole eastern Mediterranean coast will be reached by the tsunami waves. The strongest effects are predicted along south-western Turkey, Rhodes, southern Aegean and Crete, eastern Libya and Egypt. No large tsunami effects are expected in the western Mediterranean.

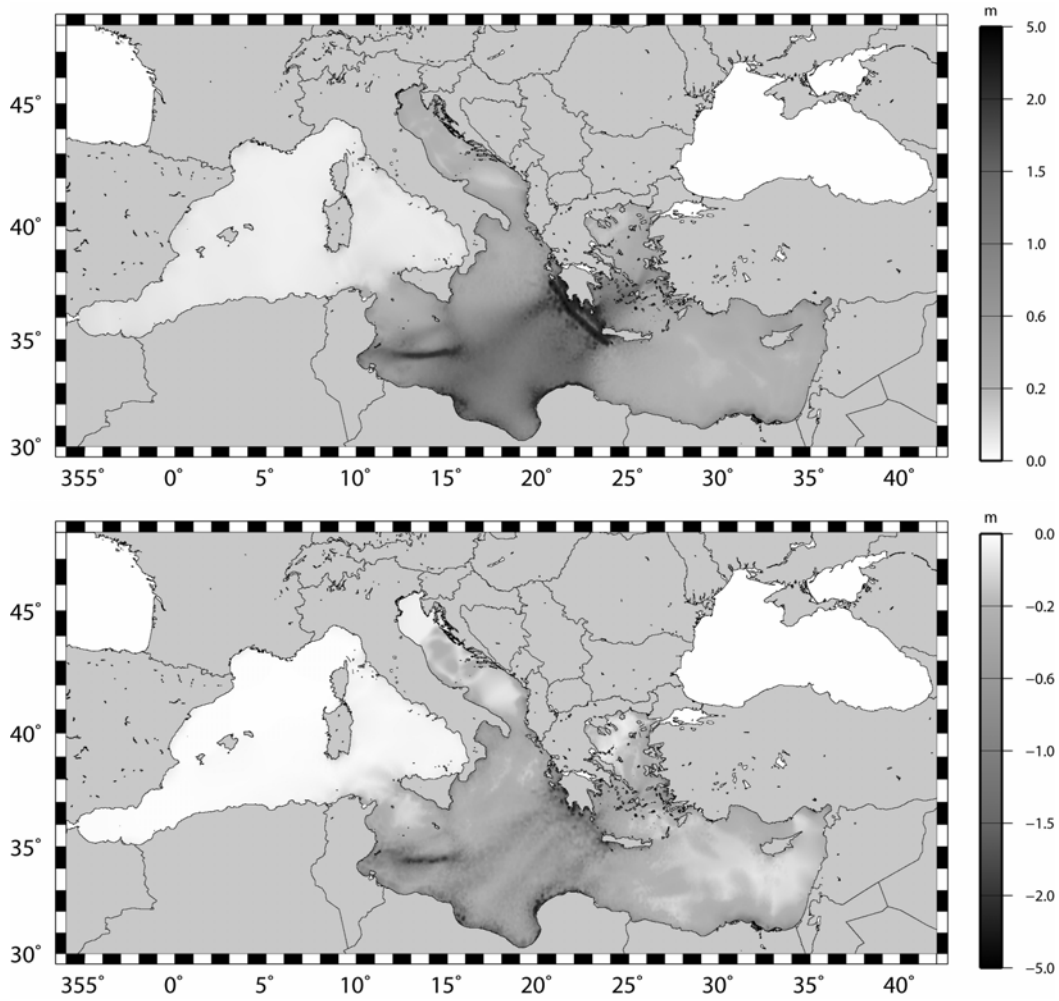


Fig. 9 Extreme water elevation fields computed for the western Hellenic Arc scenario

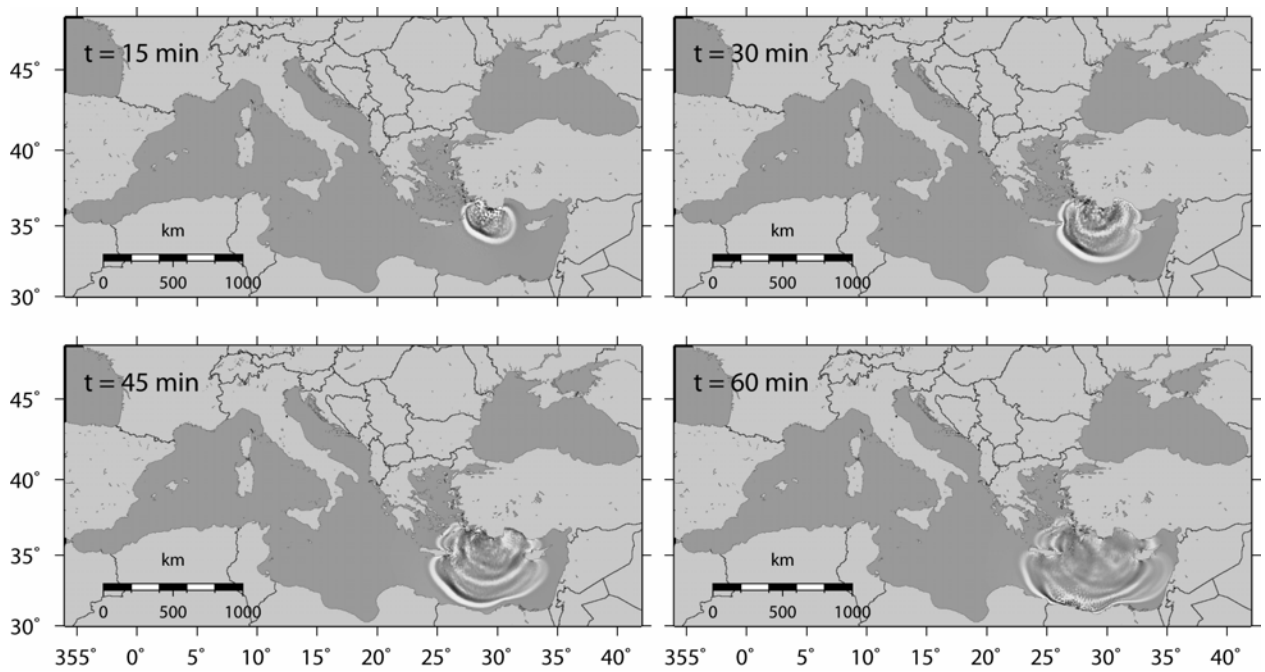


Fig. 10 Snapshots of the tsunami elevation fields computed for the eastern Hellenic Arc scenario

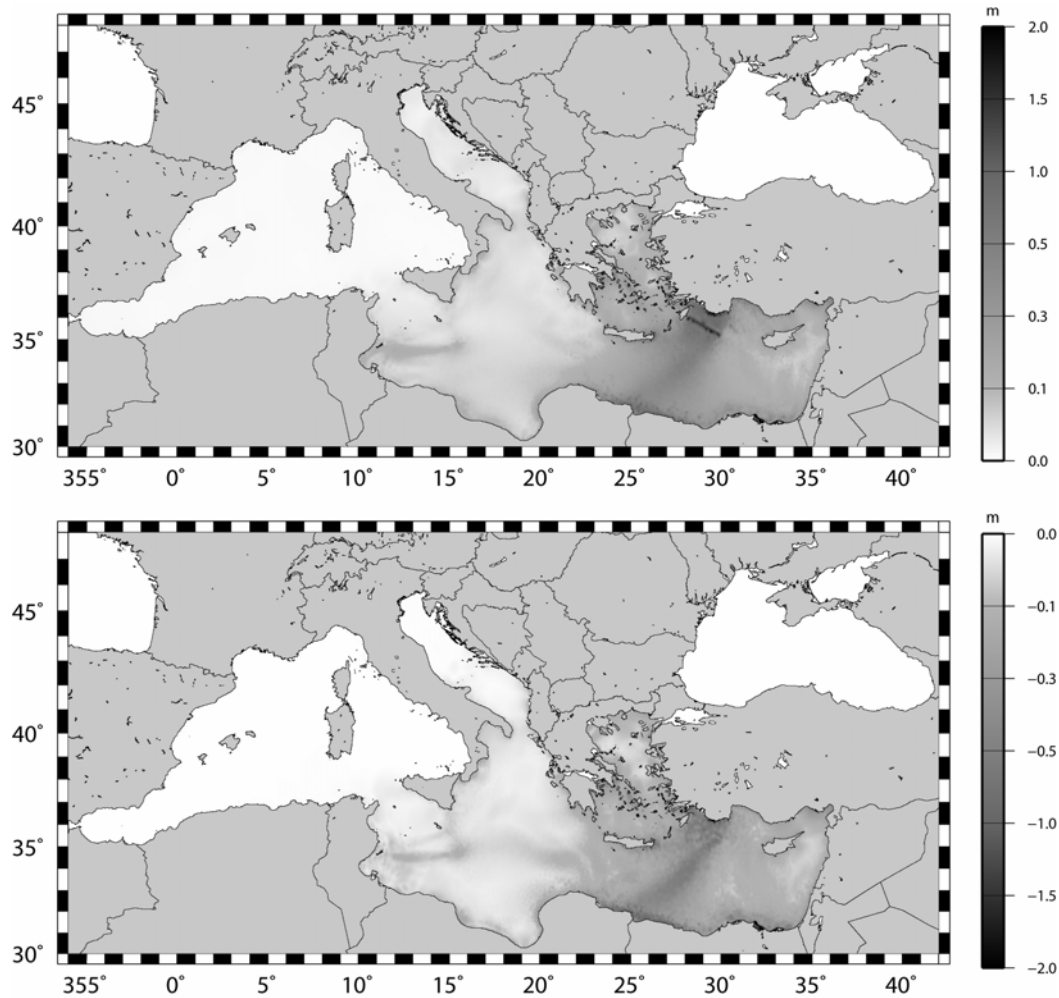


Fig. 11 Extreme water elevation fields computed for the eastern Hellenic Arc scenario

CONCLUSIONS

We examined four different scenarios of earthquake-induced tsunamis in the Mediterranean Sea. We took into account hypothetical earthquake faults placed in the western, central and eastern section of the basin, with magnitudes equal to or slightly larger than the strongest event known to have occurred in historical times in each region. We computed numerically the ensuing tsunamis and commented on their basic properties. All sources are placed very close to the coast, which is a typical feature of most sources of the Mediterranean. We have considered mega-sources, that is, sources that are characterised by the largest possible magnitudes for each region. This approximation is acceptable for the present study, which is the first attempt to explore Mediterranean scenarios, but needs to be better refined in future investigations.

The first finding is that these mega-sources are capable to produce tsunamis that share the double features of being local events and trans-Mediterranean events, in that they affect the nearest coasts as well as the remote ones. Most importantly, local coasts are attacked in a very short time, as is evident from the 15-minute snapshots portrayed in the paper. Moreover, in one hour or so, tsunamis cross the basin and hit the remote coasts opposite to the source (namely, France and Liguria, Italy for the Algerian source; Greece, Tunisia and Libya for the eastern Sicily source; Italy and northern Africa for the Hellenic Arc sources).

These propagation features are quite relevant and pose important requirements to the design of a proper TEWS for the Mediterranean in terms of response time. Devising a TEWS capable of accurate tsunami detection and of correctly forecasting tsunami impact in one hour time is useless for the Mediterranean, since most of the disastrous action has been completed by that time, and indeed most of damage on local coasts is expected to be complete within 15 minutes. It is not so for large oceans where

tsunamis takes several hours to cross the basin and to hit remote island or mainland coasts. The present TEWS practice of the Pacific Tsunami Warning Centre (PTWC) in the Pacific Ocean is to issue a first alert bulletin within 15-20 minutes and, in case of need, to issue a second refined bulletin within about one hour; though it must be improved to defend local coasts, this is considered an acceptable performance to protect remote countries. The 2004 Indian Ocean tsunami hit Sumatra coasts in the first half an hour of propagation, but took at least two hours to hit lethally the Thai coasts and more than three hours to flood eastern India and Sri Lanka. Therefore, the reaction time requirement is far more crucial for the Mediterranean Sea than for the Pacific Ocean and the Indian Ocean, and this means that the TEWS for the Mediterranean region cannot be simply a copy of the TEWS that is in place in the Pacific or of the TEWS that is being implemented in the Indian Ocean, but must have peculiar characteristics in terms of timely detection, fast signal communication, and rapid dissemination of the alert and warning messages, as well as in terms of organisation and efficiency of the national and super-national civil protection services.

As a final consideration, our attention in this paper focussed on the time needed for the first tsunami signals to reach the remote coasts, but indeed deeper attention should be paid in a future study to the long-term features of the tsunami propagation for each scenario, in order to evaluate the expected total duration of the phenomena, the characteristic periods, the relative amplitude of the wave packets and the role of edge waves. A precious hint comes from the study by Pelinovsky et al. (2002), whose attention and conclusions regarded exclusively the western Mediterranean, and in particular, the effects along the French and Ligurian coasts of locally and remotely generated tsunamis. For that particular case, the authors pointed out that several groups of tsunami waves are expected to attack the coasts, with the highest amplitudes not necessarily associated with the first arrivals. Furthermore, sea-level oscillations remain significant for several hours after the earthquake, which represents another important issue in tsunami warning.

ACKNOWLEDGMENTS

This research was funded by the Italian Ministero dell'Istruzione, dell'Università e della Ricerca (MIUR) and by the Istituto Nazionale di Geofisica e di Vulcanologia (INGV), Rome, Italy.

REFERENCES

1. Ambraseys, N.N. (1962). "Data for Investigation of Seismic Sea Waves in the Eastern Mediterranean", *Bulletin of the Seismological Society of America*, Vol. 52, No. 4, pp. 895-913.
2. Argnani, A. and Bonazzi, C. (2005). "Malta Escarpment Fault Zone Offshore Eastern Sicily: Pliocene-Quaternary Tectonic Evolution Based on New Multichannel Seismic Data", *Tectonics*, Vol. 24, No. 4, pp. TC4009/1-12.
3. Argnani, A., Bonazzi, C. and the MESC 2001 Crew (2002). "Tectonics of Eastern Sicily Offshore: Preliminary Results from the MESC 2001 Marine Seismic Cruise", *Bollettino di Geofisica Teorica e Applicata*, Vol. 43, No. 3-4, pp. 177-193.
4. Benetatos, C., Kiratzi, A., Papazachos, C. and Karakaisis, G. (2004). "Focal Mechanisms of Shallow and Intermediate Depth Earthquakes along the Hellenic Arc", *Journal of Geodynamics*, Vol. 37, pp. 253-296.
5. Bianca, M., Monaco, C., Tortorici, L. and Cernobori, L. (1999). "Quaternary Normal Faulting in Southeastern Sicily (Italy): A Seismic Source for the 1693 Large Earthquake", *Geophysical Journal International*, Vol. 139, No. 2, pp. 370-394.
6. Bouhadad, Y., Nour, A., Slimani, A., Laouami, N. and Belhai, D. (2004). "The Boumerdes (Algeria) Earthquake of May 21, 2003 ($M_w = 6.8$): Ground Deformation and Intensity", *Journal of Seismology*, Vol. 8, No. 4, pp. 497-506.
7. Bounif, A., Dorbath, C., Ayadi, A., Meghraoui, M., Beldjoudi, H., Laouami, N., Frogneux, M., Slimani, A., Alasset, P.J., Kharroubi, A., Ousadou, F., Chikh, M., Harbi, A., Larbes, S. and Maouche, S. (2004). "The 21 May 2003 Zemmouri (Algeria) Earthquake M_w 6.8: Relocation and Aftershock Sequence Analysis", *Geophysical Research Letters*, Vol. 31, No. 19, pp. L19606/1-4.
8. Braunmiller, J. and Bernardi, F. (2005). "The 2003 Boumerdes, Algeria Earthquake: Regional Moment Tensor Analysis", *Geophysical Research Letters*, Vol. 32, No. 6, pp. L06305/1-4.

9. Carminati, E. and Doglioni, C. (2004). "Mediterranean Tectonics" in "Encyclopedia of Geology (edited by R.C. Selley, L.R.M. Cocks and I.R. Plimer)", Elsevier, Amsterdam, The Netherlands.
10. Delouis, B., Vallée, M., Meghraoui, M., Calais, E., Maouche, S., Lammali, K., Mahsas, A., Briole, P., Benhamouda, F. and Yelles, K. (2004). "Slip Distribution of the 2003 Boumerdes-Zemmouri Earthquake, Algeria, from Teleseismic, GPS, and Coastal Uplift Data", *Geophysical Research Letters*, Vol. 31, No. 18, pp. L18607/1-4.
11. Déverchère, J., Yelles, K., Domzig, A., Mercier de Lépinay, B., Bouillin, J.-P., Gaullier, V., Bracène, R., Calais, E., Savoye, B., Kherroubi, A., Le Roy, P., Pauc, H. and Dan, G. (2005). "Active Thrust Faulting Offshore Boumerdes, Algeria, and its Relations to the 2003 M_w 6.9 Earthquake", *Geophysical Research Letters*, Vol. 32, No. 4, pp. L04311/1-5.
12. Di Luccio, F., Pino, N.A. and Thio, H.K. (2003). "A Study of Regional Waveform Calibration in the Eastern Mediterranean", *Geophysical Research Letters*, Vol. 30, No. 11, pp. GL016438/1-4.
13. Dominey-Howes, D. (2002). "Documentary and Geological Records of Tsunamis in the Aegean Sea Region of Greece and Their Potential Value to Risk Assessment and Disaster Management", *Natural Hazards*, Vol. 25, No. 3, pp. 195-224.
14. El-Sayed, A., Romanelli, F. and Panza, G. (2000). "Recent Seismicity and Realistic Waveforms Modeling to Reduce the Ambiguities about the 1303 Seismic Activity in Egypt", *Tectonophysics*, Vol. 328, No. 3, pp. 341-357.
15. Faccenna, C., Jolivet, L., Piromallo, C. and Morelli, A. (2003). "Subduction and the Depth of Convection in the Mediterranean Mantle", *Journal of Geophysical Research*, Vol. 108, No. B2, pp. JB001690/1-13.
16. Goes, S., Giardini, D., Jenny, S., Hollenstein, C., Kahle, H.-G. and Geiger, A. (2004). "A Recent Tectonic Reorganization in the South-central Mediterranean", *Earth and Planetary Science Letters*, Vol. 226, No. 3-4, pp. 335-345.
17. Guidoboni, E. and Comastri, A. (1997). "The Large Earthquake of 8 August 1303 in Crete: Seismic Scenario and Tsunami in the Mediterranean Area", *Journal of Seismology*, Vol. 1, No. 1, pp. 55-72.
18. Harbi, A., Benouar, D. and Benhallou, H. (2003a). "Re-appraisal of Seismicity and Seismotectonics in the North-Eastern Algeria, Part I: Review of Historical Seismicity", *Journal of Seismology*, Vol. 7, No. 1, pp. 115-136.
19. Harbi, A., Maouche, S. and Benhallou, H. (2003b). "Re-appraisal of Seismicity and Seismotectonics in the North-Eastern Algeria, Part II: 20th Century Seismicity and Seismotectonics Analysis", *Journal of Seismology*, Vol. 7, No. 2, pp. 221-234.
20. Hebert, H. and Alasset, P.J. (2003). "The Tsunami Triggered by the 21 May 2003 Algiers Earthquake", *EMSC Newsletter, Centre Sismologique Euro-Méditerranéen*, Vol. 20, pp. 10-12.
21. Henares, J., López Casado, C., Sanz de Galdeano, C., Delgado, J. and Peláez, J.A. (2003). "Stress Fields in the Iberian-Maghrebi Region", *Journal of Seismology*, Vol. 7, No. 1, pp. 65-78.
22. Laigle, M., Sachpazi, M. and Hirn, A. (2004). "Variation of Seismic Coupling with Slab Detachment and Upper Plate Structure along the Western Hellenic Subduction Zone", *Tectonophysics*, Vol. 391, pp. 85-95.
23. Le Pichon, X., Lallemand, S.J., Chamot-Rooke, N., Lemeur, D. and Pascal, G. (2002). "The Mediterranean Ridge Backstop and the Hellenic Nappes", *Marine Geology*, Vol. 186, No. 1-2, pp. 111-125.
24. Mantovani, E., Cenni, N., Albarello, D., Viti, M., Babbucci, D., Tamburelli, C. and D'Onza, F. (2001). "Numerical Simulation of the Observed Strain Field in the Central-Eastern Mediterranean Region", *Journal of Geodynamics*, Vol. 31, No. 5, pp. 519-556.
25. Marone, F., van der Meijde, M., van der Lee, S. and Giardini, D. (2003). "Joint Inversion of Local, Regional and Teleseismic Data for Crustal Thickness in the Eurasia-Africa Plate Boundary Region", *Geophysical Journal International*, Vol. 154, No. 2, pp. 499-514.
26. Marone, F., van der Lee, S. and Giardini, D. (2004). "Three-Dimensional Upper-Mantle S-Velocity Model for the Eurasia-Africa Plate Boundary Region", *Geophysical Journal International*, Vol. 158, No. 1, pp. 109-130.

27. McClusky, S., Balassanian, S., Barka, A., Demir, C., Ergintav, S., Georgiev, I., Gurkan, O., Hamburger, M., Hurst, K., Kahle, H., Kastens, K., Kekelidze, G., King, R., Kotzev, V., Lenk, O., Mahmoud, S., Mishin, A., Nadariya, M., Ouzounis, A., Paradissis, D., Peter, Y., Prilepin, M., Reilinger, R., Sanli, I., Seeger, H., Tealeb, A., Toksöz, M.N. and Veis, G. (2000). "Global Positioning System Constraints on Plate Kinematics and Dynamics in the Eastern Mediterranean and Caucasus", *Journal of Geophysical Research*, Vol. 105, No. B3, pp. 5695-5720.
28. McCoy, F.W. and Heiken, G. (2000). "Tsunami Generated by the Late Bronze Age Eruption of Thera (Santorini), Greece", *Pure and Applied Geophysics*, Vol. 157, No. 6-8, pp. 1227-1256.
29. Meghraoui, M., Maouche, S., Chema, B., Cakir, Z., Aoudia, A., Harbi, A., Alasset, P.-J., Ayadi, A., Bouhadad, Y. and Benhamouda, F. (2004). "Coastal Uplift and Thrust Faulting Associated with the $M_w = 6.8$ Zemmouri (Algeria) Earthquake of 21 May, 2003", *Geophysical Research Letters*, Vol. 31, No. 19, pp. L19605/1-4.
30. Minoura, K., Imamura, F., Kuran, U., Nakamura, T., Papadopoulos, G.A., Takahashi, T. and Yalçiner, A.C. (2000). "Discovery of Minoan Tsunami Deposits", *Geology*, Vol. 28, No. 1, pp. 59-62.
31. Okada, Y. (1992). "Internal Deformation due to Shear and Tensile Faults in a Half-Space", *Bulletin of the Seismological Society of America*, Vol. 82, No. 2, pp. 1018-1040.
32. Papadopoulos, G.A. (2002). "Tsunamis in the East Mediterranean: A Catalogue for the Area of Greece and Adjacent Seas", *Proceedings of the International Workshop on Tsunami Risk Assessment beyond 2000: Theory, Practice and Plans*, Moscow, Russia, pp. 34-42.
33. Papazachos, B.C. (1996). "Large Seismic Faults in the Hellenic Arc", *Annali di Geofisica*, Vol. 39, pp. 891-903.
34. Papazachos, B.C., Papaioannou, C.A., Papazachos, C.B. and Savvaidis, A.S. (1999). "Rupture Zones in the Aegean Region", *Tectonophysics*, Vol. 308, No. 1, pp. 205-221.
35. Papazachos, B.C., Karakostas, V.G., Papazachos, C.B. and Scordilis, E.M. (2000a). "The Geometry of the Wadati-Benioff Zone and Lithospheric Kinematics in the Hellenic Arc", *Tectonophysics*, Vol. 319, No. 4, pp. 275-300.
36. Papazachos, B.C., Comninakis, P.E., Karakaisis, G.F., Karakostas, B.G., Papaioannou, C.A., Papazachos, C.B. and Scordilis, E.M. (2000b). "A Catalogue of Earthquakes in Greece and Surrounding Area for the Period 550 B.C.-1999", *Publication of Geophysical Laboratory, University of Thessaloniki, Thessaloniki, Greece*.
37. Papazachos, B.C., Karakaisis, G.F., Papazachos, C.B. and Scordilis, E.M. (2006). "Perspectives for Earthquake Prediction in the Mediterranean and Contribution of Geological Observations", *Journal of the Geological Society* (in press).
38. Pelinovsky, E., Kharif, C., Riabov, I. and Francius, M. (2002). "Modelling of Tsunami Propagation in the Vicinity of the French Coast of the Mediterranean", *Natural Hazards*, Vol. 25, No. 2, pp. 135-159.
39. Piatanesi, A. and Tinti, S. (2002). "Numerical Modeling of the September 8, 1905 Calabrian (Southern Italy) Tsunami", *Geophysical Journal International*, Vol. 150, No. 1, pp. 271-284.
40. Semmane, F., Campillo, M. and Cotton, F. (2005). "Fault Location and Source Process of the Bumerdes, Algeria, Earthquake Inferred from Geodetic and Strong Motion Data", *Geophysical Research Letters*, Vol. 32, No. 1, pp. L01305/1-4.
41. Sirovich, L. and Pettenati, F. (2001). "Test of Source-Parameter Inversion of the Intensities of a 54,000-Death Shock of the Seventeenth Century in Southeastern Sicily", *Bulletin of the Seismological Society of America*, Vol. 91, pp. 792-811.
42. Stiros, S.C. (2001). "The AD 365 Crete Earthquake and Possible Seismic Clustering during the Fourth to Sixth Centuries AD in the Eastern Mediterranean: A Review of Historical and Archaeological Data", *Journal of Structural Geology*, Vol. 23, No. 2, pp. 545-562.
43. Stiros, S.C. and Papageorgiou, S. (2001). "Seismicity of Western Crete and the Destruction of the Town of Kisamos at AD 365: Archaeological Evidence", *Journal of Seismology*, Vol. 5, No. 3, pp. 381-397.
44. Synolakis, C.E. (1991). "Tsunami Runup on Steep Slopes: How Good Linear Theory Really is", *Natural Hazards*, Vol. 4, No. 2-3, pp. 221-234.

45. Tanioka, Y. and Satake, K. (1996). "Tsunami Generation by Horizontal Displacement of Ocean Bottom", *Geophysical Research Letters*, Vol. 23, No. 8, pp. 861-864.
46. Tinti, S. and Armigliato, A. (1999). "Seismic Displacements of Non-Flat Sea Floor in Tsunami Generation: Application to the 1693 Case in SE Sicily, Italy", *Proceedings of International Conference on Tsunamis*, Paris, France, pp. 225-245.
47. Tinti, S. and Armigliato, A. (2003). "The Use of Scenarios to Evaluate Tsunami Impact in South Italy", *Marine Geology*, Vol. 199, No. 3-4, pp. 221-243.
48. Tinti, S. and Bortolucci, E. (1999). "Strategies of Optimal Grid Generation for Finite-Element Tsunami Models", *Proceedings of International Conference on Tsunamis*, Paris, France, pp. 269-294.
49. Tinti, S., Gavagni, I. and Piatanesi, A. (1994). "A Finite-Element Numerical Approach for Modelling Tsunamis", *Annali di Geofisica*, Vol. 37, pp. 1009-1026.
50. Tinti, S., Baptista, M.A., Harbitz, C.B. and Maramai, A. (1999). "The Unified European Catalogue of Tsunamis: A GITEC Experience", *Proceedings of International Conference on Tsunamis*, Paris, France, pp. 84-99.
51. Tinti, S., Maramai, A. and Graziani, L. (2001a). "A New Version of the European Tsunami Catalogue: Updating and Revision", *Natural Hazards and Earth System Sciences*, Vol. 1, pp. 255-262.
52. Tinti, S., Armigliato, A. and Bortolucci, E. (2001b). "Contribution of Tsunami Data Analysis to Constrain the Seismic Source: The Case of the 1693 Eastern Sicily Earthquake", *Journal of Seismology*, Vol. 5, No. 1, pp. 41-61.
53. Tinti, S., Maramai, A. and Graziani, L. (2004). "The New Catalogue of Italian Tsunamis", *Natural Hazards*, Vol. 33, No. 3, pp. 439-465.
54. Vannucci, G. and Gasperini, P. (2004). "The New Release of the Database of Earthquake Mechanisms of the Mediterranean Area (EMMA Version 2)", *Annali di Geofisica*, Supplement to Vol. 47, No. 1, pp. 307-334.
55. Yelles, K., Lammali, K., Mahsas, A., Calais, E. and Briole, P. (2004). "Coseismic Deformation of the May 21st, 2003, $M_w = 6.8$ Boumerdes Earthquake, Algeria, from GPS measurements", *Geophysical Research Letters*, Vol. 31, No. 13, pp. L13610/1-5.